

Wavepacket Correlation Function Approach for Nonadiabatic Reactions: Quasi-Jahn-Teller Model

Heesoo Park, Changkyun Shin,* and Seokmin Shin*

Seoul National University, Seoul 151-747, Korea. *E-mail: sshin@smu.ac.kr (S. Shin); sisid1@smu.ac.kr (C. Shin)
Received October 25, 2013, Accepted December 11, 2013

Time-dependent formulations of the reactive scattering theory based on the wavepacket correlation functions with the Møller wavepackets for the electronically nonadiabatic reactions are presented. The calculations of state-to-state reactive probabilities for the quasi-Jahn-Teller scattering model system were performed. The conical intersection (CI) effects are investigated by comparing the results of the two-surface nonadiabatic calculations and the single surface adiabatic approximation. It was found that the results of the two-surface nonadiabatic calculations show interesting features in the reaction probability due to the conical intersection. Single surface adiabatic calculations with extended Born-Oppenheimer approximation using simple wavepacket phase factor was found to be able to reproduce the CI effect semi-quantitatively, while the single surface calculations with the usual adiabatic approximation cannot describe the scattering process for the Jahn-Teller model correctly.

Key Words : Wavepacket correlation function, Nonadiabatic reaction, Conical intersection

Introduction

Reactive scattering studies have been successful for 3- and 4-atom bimolecular reactions.^{1,2} These studies were based on a single electronically adiabatic PES potential energy surface (PES) obtained *a priori* using the Born-Oppenheimer approximation. Time-dependent methods possess some attractive features for large-scale numerical calculations, which has been used for the possible extension of scattering studies to reactions involving polyatomic molecules.^{2,3} It has also been recognized that the time-dependent wavepacket approach can provide direct information on the underlying reaction dynamics. Additionally, time-dependent studies can be used to develop approximate theories such as semiclassical, mixed quantum/classical, or time-dependent self-consistent-field (TDSCF) methods.

Reactions can occur on multiple electronic states, which require the inclusion of nonadiabatic effects. However, theoretical studies of reaction dynamics on multiple PESs have been rather limited. Only a few quantum mechanical scattering studies have been attempted so far.⁴⁻⁶ Even for low enough energies such that upper electronic states cannot be populated, the presence of electronic degeneracy has been found to affect molecular dynamics including scattering processes.^{7,8} In order to reveal much richer dynamical phenomena, one needs time-dependent studies on general reactive scattering processes involving multiple electronic states.

Nonadiabatic processes are ubiquitous in reactions involving polyatomic molecules.^{9,10} The conical interaction (CI) between Born-Oppenheimer potential energy surfaces is an important example of such nonadiabatic effect,^{11,12} as demonstrated by Herzberg and Longuet-Higgins.^{13,14} The possible effects of CI on scattering processes have been extensively studied.^{7,15,16} For systems with three identical atoms, the

Jahn-Teller (JT) effect is the most well-known phenomena.^{14,17} Baer *et al.* extended the Jahn-Teller model, which was originally devised for bound systems, to a scattering process.¹⁸ Using a simple two-dimensional quasi-JT model, the effect on the symmetry of the nuclear wavefunctions due to CI was examined by time-dependent scattering calculations. Adhikari and Billing addressed the same problem using the same model with a time-dependent wavepacket approach.¹⁹

In this paper we present an extension of the wavepacket correlation function formulation with the Møller operator to the scattering in the quasi-Jahn-Teller model system. The purpose of the present study is to illustrate the application of a time-dependent approach to electronically nonadiabatic reactions. In order to obtain the state-to-state reaction probability, we used the correlation function formulations developed by Tannor and coworkers.²⁰⁻²⁶ A time-dependent reactive scattering formulation in which the individual S-matrix elements or the cumulative reaction probabilities were obtained from time-correlation functions between reactant and product wave packets with appropriate boundary conditions. Similar formulations based on time-dependent wavepackets have also been introduced by others.^{27,28} Recently, we proposed a simple extension of the wavepacket correlation function formulation to electronically nonadiabatic reactions, which was applied to simple model reactions.²⁹

Theory and Model

Adiabatic and Diabatic Representations. The relation between the adiabatic and diabatic representations is well known. The detailed descriptions of the adiabatic and diabatic representations in scattering problems are given in previous works.^{8,30} Here, we briefly summarize relevant relations.

In the adiabatic representation, the equation for nuclear wavefunction χ given in the form:

$$-\frac{\hbar^2}{2m} \left[\nabla^2 \chi(i) + 2 \sum_{j \neq i} \nabla \chi(j) \langle \phi(i) | \nabla \phi(j) \rangle + \sum_{j \neq i} \chi(j) \langle \phi(i) | \nabla^2 \phi(j) \rangle \right] + V \chi(i) = E \chi(i). \quad (1)$$

For two-surface case, Eq. (1) is given by simple matrix form as

$$\begin{pmatrix} \nabla_1^2 + V_1 - E & 2 \langle \phi(1) | \nabla \phi(2) \rangle \nabla_1 \\ & + \langle \phi(1) | \nabla^2 \phi(2) \rangle \\ 2 \langle \phi(2) | \nabla \phi(1) \rangle \nabla_2 & \nabla_2^2 + V_2 - E \\ + \langle \phi(2) | \nabla^2 \phi(1) \rangle & \end{pmatrix} \times \begin{pmatrix} \chi(1) \\ \chi(2) \end{pmatrix} = 0. \quad (2)$$

The adiabatic representation can be transformed into the diabatic representation where the nuclear wavefunction satisfies the following equation:

$$\begin{pmatrix} \nabla_1^2 + V_1 - E & V_{12} \\ V_{21} & \nabla_2^2 + V_2 - E \end{pmatrix} \begin{pmatrix} d(1) \\ d(2) \end{pmatrix} = 0 \quad (3)$$

with

$$\begin{pmatrix} d(1) \\ d(2) \end{pmatrix} = T^{-1} \begin{pmatrix} \chi(1) \\ \chi(2) \end{pmatrix}, \quad (4a)$$

and

$$\begin{pmatrix} \nabla_1^2 + V_1 - E & V_{12} \\ V_{21} & \nabla_2^2 + V_2 - E \end{pmatrix} = T^{-1} \begin{pmatrix} \nabla_1^2 + V_1 - E & 2A \nabla_1 + B \\ 2A \nabla_2 + B & \nabla_2^2 + V_2 - E \end{pmatrix} T. \quad (4b)$$

where $A = \langle \phi(1) | \nabla \phi(2) \rangle$, $B = \langle \phi(1) | \nabla^2 \phi(2) \rangle$.

The transformation matrix is given by

$$T = \begin{pmatrix} \cos \alpha & -\sin \alpha \\ \sin \alpha & \cos \alpha \end{pmatrix}. \quad (5)$$

In two-dimensional problem, one can use either Cartesian coordinates or polar coordinates. They are related by

$x = q \cos \theta$ and $y = q \sin \theta$ with $\theta = \tan^{-1} \left(\frac{y}{x} \right)$. In this case,

the transformation angle α is given simply by $\alpha = \frac{\theta}{2}$.

Correlation Function Formulation of S-matrix. S-matrix

elements can be defined by the overlap of the eigenfunctions in the reactant and product regions of the scattering system: $S_{\beta\alpha}(E) = \langle \Psi_{\beta}^{-}(E) | \Psi_{\alpha}^{+}(E) \rangle$. Here α and β are internal quantum numbers of reactant and product channels, respectively. A lot of studies have examined efficient methods for calculating S-matrix elements. For example, one can calculate flux passing through the dividing surface of the reaction coordinates.²⁹

$$S_{\beta\alpha}(E) = \frac{\int dt \langle \psi_{\beta}(t) | F | \psi_{\alpha}(t) \rangle}{\int_{k_i}^{k_f} dk \eta(k)}. \quad (6)$$

Consider a wavepacket located at the asymptotic reactant channel having a momentum of incoming direction initially and propagated to the interaction scattering region. Then it is propagated back to the asymptotic reactant channel or moved to the asymptotic product channel at the final time. The incoming and outgoing wavepackets can be represented with its asymptotic eigenfunctions as basis:

$$|\Phi_{\alpha}^{+}\rangle = \int_0^{\infty} \eta_{\alpha}(E) |\psi_{\alpha}^{+}(E)\rangle dE, \quad (7a)$$

$$|\Phi_{\beta}^{-}\rangle = \int_0^{\infty} \zeta_{\beta}(E) |\psi_{\beta}^{-}(E)\rangle dE. \quad (7b)$$

The formula of the scattering matrix elements $S_{\beta\alpha}$ is easily obtained as below:

$$|\eta_{\alpha}(E)|^2 = \frac{1}{2\pi} \int_{-\infty}^{\infty} \langle \Phi_{\alpha}^{+} | e^{-iHt} | \Phi_{\alpha}^{+} \rangle e^{iEt} dt, \quad (8a)$$

$$|\zeta_{\beta}(E)|^2 = \frac{1}{2\pi} \int_{-\infty}^{\infty} \langle \Phi_{\beta}^{-} | e^{-iHt} | \Phi_{\beta}^{-} \rangle e^{iEt} dt, \quad (8b)$$

$$S_{\beta\alpha} = \frac{1}{2\pi \zeta_{\beta}^{*}(E) \eta_{\alpha}(E)} \int_{-\infty}^{\infty} \langle \Phi_{\beta}^{-} | e^{-iHt} | \Phi_{\alpha}^{+} \rangle e^{iEt} dt. \quad (9)$$

Tannor and coworkers introduced the new formula of scattering matrix elements, using Fourier transform of time correlation function, which is equivalent with the following flux-operation formula.⁹⁻¹⁵

$$|S_{\beta\alpha}(E)|^2 = \frac{\left| \int_{-\infty}^{\infty} \langle \psi_{\beta}^{-} | e^{-iHt} | \psi_{\alpha}^{+} \rangle e^{iEt} dt \right|^2}{\left| \int_{-\infty}^{\infty} \langle \psi_{\alpha}^{-} | e^{-iHt} | \psi_{\alpha}^{+} \rangle e^{iEt} dt \right| \left| \int_{-\infty}^{\infty} \langle \psi_{\beta}^{-} | e^{-iHt} | \psi_{\beta}^{-} \rangle e^{iEt} dt \right|}. \quad (10)$$

Calculation Details. At $t = 0$, one can use so-called ‘‘Møller wavepacket’’ for Φ_{α}^{+} and Φ_{β}^{-} . Initially it is set in the interaction region of the system and propagated to its asymptotic region without interaction potential, then it is propagated back until $t = 0$ to the interaction region with full potential. By using Møller wavepackets, one can reduce the range of the coordinate and the number of grid points for propagation because they are defined in the interaction region. Since the free Hamiltonian H_0 and full Hamiltonian H are canceled out in the asymptotic channels, the length of the asymptotic region can also be reduced. For the calculation of

correlation function, wavepackets, after they pass through fixed reference wavepacket, are propagated out until the value of correlation function converges to zero. It is noted that taking the reference wavepacket at the center of the whole system is advantageous, effectively reducing ranges of the asymptotic channels.

The correlation function in terms of the Møller operator is written as follows:

$$C_{\beta\alpha}(t) = \langle \Phi_{\beta}^{-} | e^{-iHt} | \Phi_{\alpha}^{+} \rangle = \langle \Phi_{\beta} | \Omega_{\beta}^{+} e^{-iHt} \Omega_{\alpha}^{+} | \Phi_{\alpha} \rangle \quad (11)$$

where $\Omega_{\alpha}^{+} = \lim_{t \rightarrow -\infty} e^{iHt} e^{-iH_{\alpha}^{0}t}$ and $\Omega_{\beta}^{-} = \lim_{t \rightarrow \infty} e^{iHt} e^{-iH_{\beta}^{0}t}$.

The correlation function now becomes:

$$C_{\beta\alpha}(t) = \lim_{\substack{t' \rightarrow -\infty \\ t'' \rightarrow \infty}} \langle \Phi_{\beta} | e^{iH_{\beta}^{0}t''} e^{-iHt'} e^{-iHt} e^{iHt'} e^{-iH_{\alpha}^{0}t'} | \Phi_{\alpha} \rangle \quad (12)$$

We set initial incoming and outgoing wavepackets as Møller wavepackets in the interaction region, which is equivalent to not canceling out the 2nd and 4th factors in Eq. (12), which are $e^{-iHt'}$ and $e^{iHt'}$ respectively. In the following, we briefly describe a procedure to evaluate correlation function based on the above scheme:

- We propagate initial incoming and outgoing wavepackets in the interaction region at $t = 0$ to their asymptotic regions under the free Hamiltonian.
- We prepare initial Møller wavepackets by applying the 2nd and 4th factors in Eq. (12), *i.e.*, propagating the wavepackets in (a) back to the time $t = 0$ under the full Hamiltonian.
- For $t > 0$, correlation function is calculated by overlap

between outgoing wavepacket prepared in (b) and incoming wavepacket propagated forward in time t .

- For $t < 0$, correlation function is calculated by overlap between incoming wavepacket prepared in (b) and outgoing wavepacket propagated backward in time t .

The terms of $\eta(E)$ and $\zeta(E)$ can be derived from the autocorrelation functions of Φ_{α}^{+} and Φ_{β}^{-} , which can be calculated by the similar procedure as the above.

Assuming that the free and full Hamiltonians in the propagator include two electronic states, the time-dependent equation in adiabatic representation becomes

$$i\hbar \frac{d}{dt} \begin{pmatrix} d_1(t) \\ d_2(t) \end{pmatrix} = \mathbf{H}_d \begin{pmatrix} d_1(t) \\ d_2(t) \end{pmatrix}, \quad (13)$$

the solution of this equation is given by

$$\begin{pmatrix} d_1(t) \\ d_2(t) \end{pmatrix} = \exp(-i\mathbf{H}_d t) \begin{pmatrix} d_1(0) \\ d_2(0) \end{pmatrix} \quad (14)$$

The time-evolutions of the corresponding diabatic wavepackets can be done with split operator propagation in multiple electronic states.¹⁸

Model Potential. The potential energy surfaces are adopted from quasi-Jahn-Teller model with two degree of freedom.²⁸ Two different potential energy surfaces are distinguished by the vibration-coordinate symmetry of the ground potential surface at the intersection region. They are called as reactive double split model (RDSM) and reactive single split model (RSSM). In the present work, we will consider the RDSM model. The adiabatic potential energy surfaces are given by:

$$u_1(R, r) = \frac{1}{2}m(\omega_0 - \tilde{\omega}_1(R))^2 r^2 + Af(R, r) + g(R), \quad (15a)$$

$$u_2(R, r) = \frac{1}{2}m\omega_0^2 r^2 + (D - A)f(R, r) + D \quad (15b)$$

where $\tilde{\omega}_1(R) = \omega_1 \exp(-\frac{R}{\sigma_1})^2$ and R and r are the translational and the vibrational coordinates, respectively. The functions $f(R, r)$ and $g(R)$ for the RDSM model are:

$$f(R, r) = \exp\left(-\frac{R^2 + r^2}{\sigma^2}\right), \quad (16a)$$

$$g(r) \equiv 0 \quad (16b)$$

The corresponding diabatic potential energy surfaces are obtained by the following equations:

$$V_{11}(R, r) = \frac{1}{2}(u_1 + u_2 + (u_1 - u_2)\cos\theta), \quad (17a)$$

$$V_{12}(R, r) = \frac{1}{2}(u_2 - u_1)\sin\theta, \quad (17b)$$

$$V_{22}(R, r) = \frac{1}{2}(u_1 + u_2 + (u_2 - u_1)\cos\theta) \quad (17c)$$

The same potential parameters as the previous work by Baer and Kosloff²⁸ are used in this work. The potential

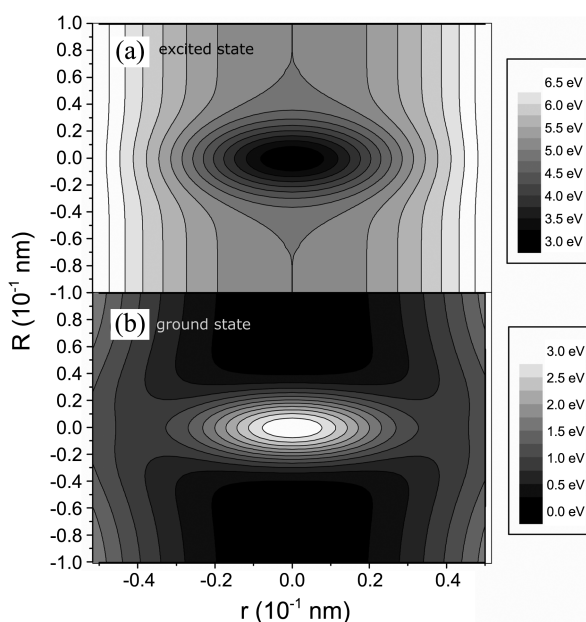


Figure 1. Contour plots for the adiabatic potential energy surfaces of the reactive double split model (RDSM): (a) the excited state and (b) the ground state. The parameters of the applied quasi-JT model are $A = 3.0$ eV and $D = 5.0$ eV.

Table 1. Parameters used in numerical calculations

Coordinate Grid			
R_{\min}, R_{\max}	± 0.2 nm	r_{\min}, r_{\max}	± 0.1 nm
$N_R \times N_r$			
Initial Wavepacket			
(R_0, r_0)	(0,0) nm	σ_R	0.05 nm
Kinetic energy	1.65 eV		
Time Propagation			
dt	1.0 au	t	± 3300 au (-80 fs \rightarrow 80 fs)

surfaces of the RDSM model are shown in Figure 1.

Results and Discussion

The initial wavepackets are constructed by choosing a Gaussian function in R and a vibrational eigenfunction in r with the initial momentum corresponding to a given kinetic energy. The parameters for the initial wavepackets and the subsequent propagation are given in Table 1. First we set the initial wavepacket in the ground adiabatic potential in the center of the system at $t = 0$, and calculated the corresponding Møller wavepackets. The initial diabatic wavepackets are shown in Figure 2, while the Møller wavepackets Φ_{α}^{+} and Φ_{β}^{-} are shown in Figure 3. It is noted that the two initial

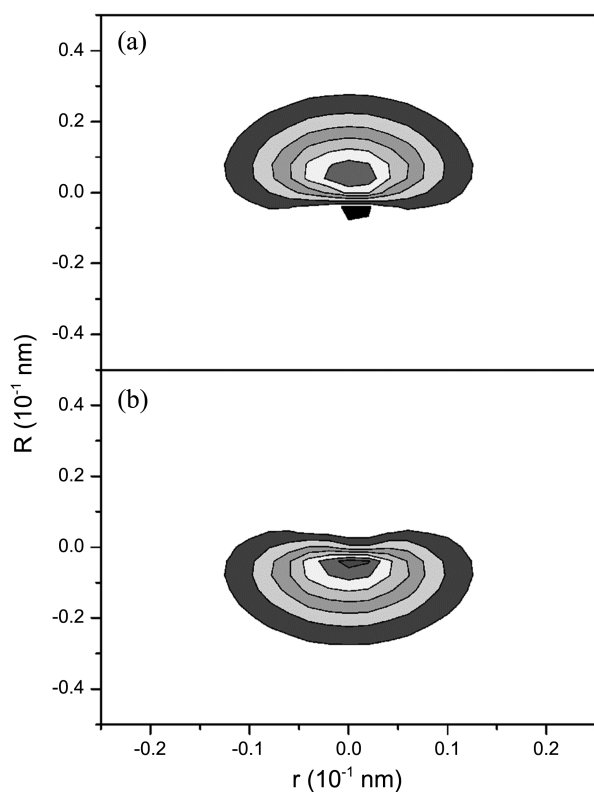


Figure 2. Contour plots for the initial wavepackets Φ_{α} in diabatic representation: (a) wavepacket for the product channel diabatic potential energy surface and (b) wavepacket for the reactant channel diabatic potential energy surface.

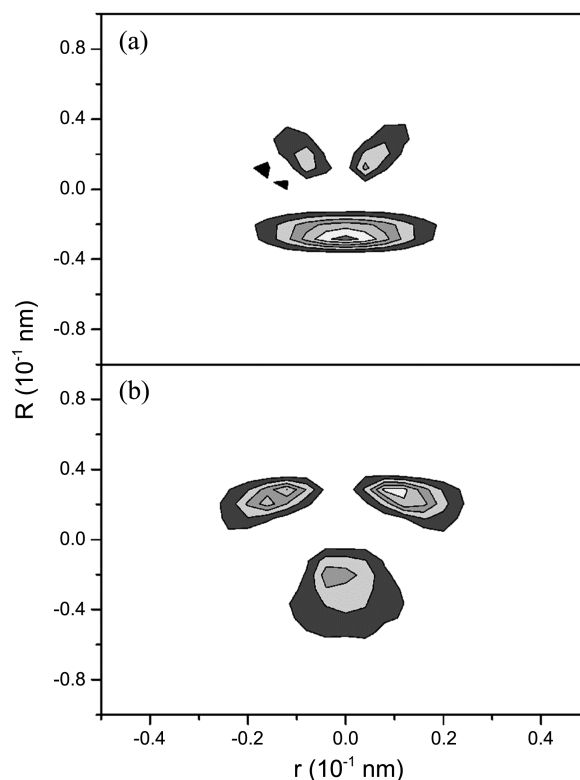


Figure 3. Contour plots of Møller wavepackets at $t = 0$ in the ground adiabatic state: (a) Φ_{α}^{+} and (b) Φ_{β}^{-} .

diabatic wavepackets were defined in the reactant and product regions, respectively, away from the conical intersection point. The Møller wavepackets are different from the diabatic wavepackets because the initial states spread through the CI due to the propagation by the Møller operator.

By analyzing the adiabatic representation of the propagated Møller wavepacket as a function of time, one can follow the dynamics of the system going from its asymptotic reactant region, through the interaction region, moving to the asymptotic product region. Considering the range of spatial grids for the numerical calculations, the time scales for the wavepacket propagation was set to be between -80 fs and 80 fs. The shape of ground adiabatic wavepacket obtained from the propagated Møller wavepacket at the product asymptotic region ($t = 72$ fs) is shown in Figure 4(a), while that at the reactant asymptotic region is shown in Figure 4(b). The diabatic wavepacket at its asymptotic past ($t = -80$ fs) is illustrated in Fig. 4(c). The evolution of the populations of adiabatic states is shown in Figure 5. The initial wavepacket was set in the interaction region of the system, thus the population was 0.5 for both the ground and excited states. As we propagated the states, the population increased up to 0.9 for the ground state, meanwhile the population reduced down to 0.1 for the excited state. Using the Møller operator, the wavepacket ($t = 0$) was constructed by applying reactant and product Møller operators Ω_{α}^{+} and Ω_{β}^{-} s, and the scattering dynamics were observed for relatively short range in time.

In the previous time-independent and time-dependent

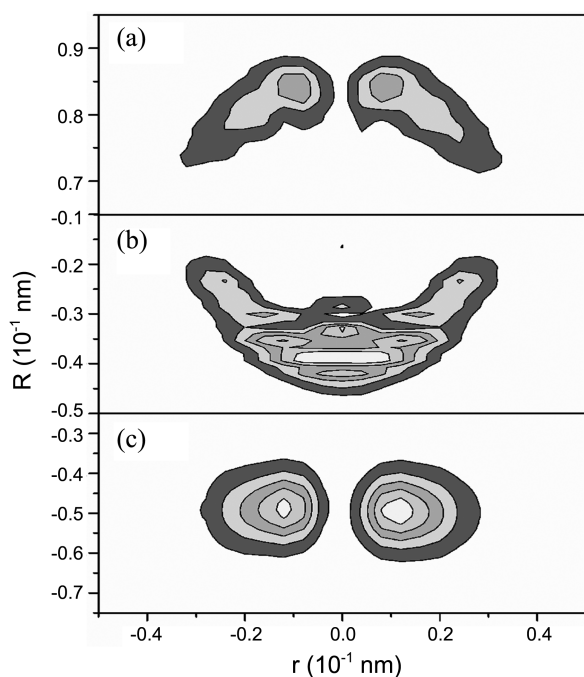


Figure 4. Contour plots of the ground state adiabatic wavepacket obtained from the propagated Møller wavepacket when $t = 72$ fs (a) at the product asymptotic region and (b) at the reactant asymptotic region. (c) A contour plot of the diabatic wavepacket at its asymptotic past ($t = -80$ fs).

studies,^{18,19} the effects of symmetry of the vibrational states were investigated with regard to the RDSM and the RSSM models. For a Jahn-Teller model, a wavepacket near the conical-intersection (CI) point is affected such that its spatial phase is inverted, whose quantitative effects are dependent on the symmetry of the system. The change in the spatial phase of wavepacket for the RDSM model leads to the corresponding changes in the state-to-state selection rule such that only even-odd transitions are allowed while even-even or odd-odd transitions were annihilated. The change of

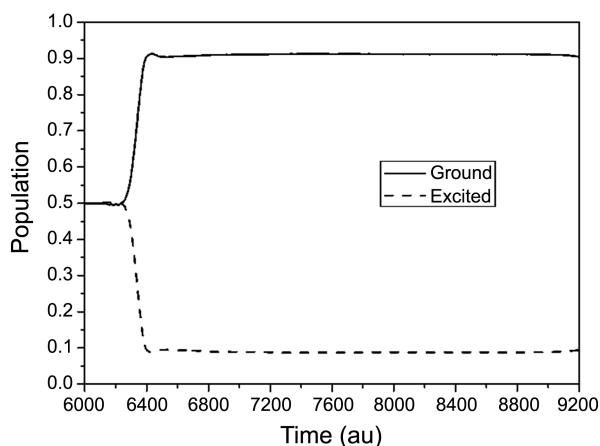


Figure 5. Populations of the ground (solid line) and the excited (dashed line) adiabatic states during the propagation of the Møller wavepacket. It is noted that $t = 6400$ au is defined to be the origin of the time ($t = 0$).

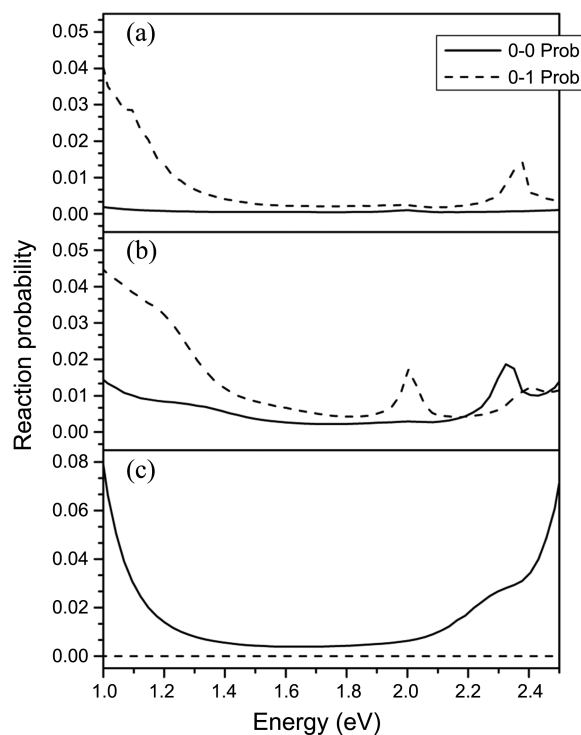


Figure 6. The state-to-state reaction probabilities, $|S_{\beta\alpha}|^2$, calculated from (a) the two-surface nonadiabatic calculations, (b) the single surface calculations with the extended BO approximation, and (c) the single surface calculations with the ordinary BO approximation for the $0 \rightarrow 0$ transition (solid line) and the $0 \rightarrow 1$ transition (dashed line).

spatial phase can be represented as an exponential term with half of the spatial polar angle according to the extended BO approximation. It was demonstrated that the results with adiabatic wavepackets multiplied with the exponential phase in the single adiabatic potential surface showed good agreements with those of the two-surface diabatic calculations.

We obtained S-matrices of the system by different methods: nonadiabatic calculation with double electronic surfaces; adiabatic approximation with the wavepacket of changed phase (extended Bohn-Oppenheimer scheme¹⁸); and adiabatic approximation with the typical wavepacket (ordinary BO scheme). The vibrational state of the reactant wavepacket Φ_α was set to 0 and that of the product packet Φ_β to 0 or 1. We calculated probabilities of $0 \rightarrow 0$ and $0 \rightarrow 1$ transitions. Figure 6 showed the transition probabilities calculated by three different methods: (a) two-surface nonadiabatic calculations, (b) single surface calculations with the extended BO approximation, and (c) single surface calculations with the ordinary BO approximation. It is noted that time-correlation functions based on the propagation of the Møller wavepackets were used in the present calculations. Compared with the previous study,²⁹ the state-to-state reaction probability with respect to the energy is found to be averaged and the S-matrix elements for lower energies seemed to be overestimated. However, a peak of the reaction probability around 2.2 to 2.4 eV for the $0 \rightarrow 1$ transition from two-surface nonadiabatic calculations is consistent with the

previous results.^{18,19,29} Main focus of the present study is to examine how salient features of nonadiabatic reactions can be described by time-dependent approaches. The results from the two-surface nonadiabatic calculations clearly show the effects of CI on the selection rules of transition probabilities, while the single surface adiabatic calculations lead to erroneous results. In fact, the symmetry properties of the transition probabilities for the single surface with the ordinary BO approximation are completely reversed from those for the two-surface nonadiabatic cases with CI. Although the wavepackets were propagated on a single surface, we observed that the main features of CI effects can be recovered by implementing the extended BO approximation. The calculations showed that the 0-1 transition probability is higher in the almost range of energy. However, these results showed quantitative differences compared with the exact two-surface calculations.

Concluding Remarks

We have extended a time-dependent formulation of quantum mechanical scattering theory to reactions on multiple electronic states. Wavepacket correlation function theory of Tannor and coworkers was applied to electronically nonadiabatic processes. It was shown that S-matrix can be calculated with a correlation function using propagation of Møller wavepackets of the system. We have applied the method to a simple two-dimensional quasi-JT (Jahn-Teller) model. It was found that the results of the two-surface nonadiabatic calculations show interesting features in the reaction probability due to the conical intersection. The single surface adiabatic calculation with the extended BO approximation was found to be able to represent the CI effect semi-quantitatively, while the single surface calculations with the usual adiabatic approximation cannot describe the scattering process for the Jahn-Teller model correctly.

It is shown that a straightforward extension of the wavepacket correlation function method to electronically nonadiabatic reactions can be constructed by the Møller formulation of scattering. The time-dependent formulation of reactive scattering theory can be cast into various forms in order to provide an improved route to the evaluation of S-matrix or cumulative reaction probabilities. Possible applications of similar modifications to our time-dependent formulation for handling reactions on multiple electronic states will be the subject of future studies. Those efforts will include the use of semiclassical wavepacket propagation and implementations

based on the ideas of quantum transition state theory.

Acknowledgments. This work was supported by the National Research Foundation of Korea (NRF) grants funded by the Korea government (MSIP): No. 2007-0056095 (CMD) and No.2012M3C1A6035358 (EDISON).

References

1. Schatz, G. C. *J. Phys. Chem.* **1996**, *100*, 12839.
2. Zhang, J. Z. H.; Dai, J.; Zhu, W. *J. Phys. Chem. A* **1997**, *101*, 2746.
3. Zhang, D. H.; Zhang, J. Z. H. In *Dynamics of Molecules and Chemical Reactions*, Wyatt, R. E., Zhang, J. Z. H., Eds.; Marcel Dekker: New York, 1996; p 231.
4. Gilbert, M.; Baer, M. *J. Phys. Chem.* **1994**, *98*, 12822.
5. Tawa, G. J.; Mielke, S. L.; Truhlar, D. G.; Schwenke, D. W. *J. Chem. Phys.* **1994**, *100*, 5751.
6. Schatz, G. C. *J. Phys. Chem.* **1995**, *99*, 7522.
7. Mead, C. A.; Truhlar, D. G. *J. Chem. Phys.* **1979**, *70*, 2284.
8. Shin, C.; Shin, S. *J. Chem. Phys.* **2000**, *113*, 6828.
9. Nakamura, H. *Nonadiabatic Transitions*; World Scientific: Singapore, 2002.
10. Jasper, A. W.; Zhu, C.; Nangia, S.; Truhlar, D. G. *Faraday Discuss.* **2004**, *127*, 1.
11. Teller, E. *J. Phys. Chem.* **1937**, *41*, 109.
12. Herzberg, G. *Molecular Spectra and Molecular Structure III. Electronic Spectra and Electronic Structure of Polyatomic Molecules*; Van Nostrand Reinhold: New York, 1966; pp 442-444.
13. Longuet-Higgins, H. C. *Proc. R. Soc. London, Ser. A* **1975**, *34*, 147.
14. Herzberg, G.; Longuet-Higgins, H. C. *Discuss. Faraday Soc.* **1963**, *35*, 77.
15. Wu, Y. M.; Lepetit, B.; Kuppermann, A. *Chem. Phys. Lett.* **1991**, *186*, 319.
16. Worth, G. A.; Cederbaum, L. S. *Annu. Rev. Phys. Chem.* **2004**, *55*, 127.
17. Englman, R. *The Jahn-Teller Effect in Molecules and Crystals*; Wiley-Interscience: New York, 1972.
18. Baer, R.; Charutz, D. M.; Kosloff, R.; Baer, M. *J. Chem. Phys.* **1996**, *105*, 9141.
19. Adhikari, S.; Billing, G. D. *J. Chem. Phys.* **1999**, *111*, 40.
20. Tannor, D. J.; Weeks, D. E. *J. Chem. Phys.* **1993**, *98*, 3884.
21. Weeks, D. E.; Tannor, D. J. *J. Chem. Phys. Lett.* **1993**, *207*, 301.
22. Garashchuk, S.; Tannor, D. *J. Chem. Phys. Lett.* **1996**, *262*, 477.
23. Garashchuk, S.; Grossmann, F.; Tannor, D. *J. Chem. Soc. Faraday Trans.* **1997**, *93*, 781.
24. Garashchuk, S.; Tannor, D. J. *J. Chem. Phys.* **1998**, *109*, 3028.
25. Garashchuk, S.; Tannor, D. J. *J. Chem. Phys.* **1999**, *110*, 2761.
26. Garashchuk, S.; Tannor, D. J. *Annu. Rev. Phys. Chem.* **2000**, *51*, 553.
27. Grossmann, F.; Heller, E. *Chem. Phys. Lett.* **1995**, *241*, 45.
28. Zhang, D. H.; Light, J. C. *J. Chem. Phys.* **1996**, *104*, 6184.
29. Yoon, Y.; Shin, C.; Shin, S. *J. Chem. Phys.* **2006**, *326*, 425.
30. Shin, S.; Light, J. C. *J. Chem. Phys.* **1994**, *101*, 2836.